Development 129, 5093-5101 (2002)
Printed in Great Britain © The Company of Biologists Limited 2002
DEV5029

DEVELOPMENT AND DISEASE

hrT is required for cardiovascular development in zebrafish

Daniel P. Szeto, Kevin J. P. Griffin and David Kimelman*

Department of Biochemistry, Box 357350, University of Washington, Seattle, WA 98195-7530, USA
*Author for correspondence (e-mail: kimelman@u.washington.edu)

Accepted 30 July 2002

SUMMARY

The recently identified zebrafish T-box gene *hrT* is expressed in the developing heart and in the endothelial cells forming the dorsal aorta. Orthologs of *hrT* are expressed in cardiovascular cells from *Drosophila* to mouse, suggesting that the function of *hrT* is evolutionarily conserved. The role of *hrT* in cardiovascular development, however, has not thus far been determined in any animal model. Using morpholino antisense oligonucleotides, we show that zebrafish embryos lacking *hrT* function have dysmorphic hearts and an absence of blood circulation. Although the early events in heart formation were normal in *hrT* morphant embryos, subsequently the hearts failed to undergo looping, and late onset defects in chamber morphology and gene expression were observed. In particular, we found that the loss of *hrT* function led to a dramatic upregulation of *tbx5*, a gene required for normal heart morphogenesis. Conversely, we show that overexpression of *hrT* causes a significant downregulation of *tbx5*, indicating that one key role of *hrT* is to regulate the levels of *tbx5*. Secondly, we found that HrT is required to inhibit the expression of the blood lineage markers *gata1* and *gata2* in the most posterior lateral plate mesoderm. Finally, we show that HrT is required for vasculogenesis in the trunk, leading to similar vascular defects to those observed in midline mutants such as *floating head*. *hrT* expression in the vascular progenitors depends upon midline mesoderm, indicating that this expression is one important component of the response to a midline-derived signal during vascular morphogenesis.

Key words: Zebrafish, *hrT*, Cardiogenesis, Dorsal aorta, *tbx5*, *fli1*, *floating head*

INTRODUCTION

The developmental roles of the T-box genes have been an area of intense research for many years (Papaioannou and Silver, 1998; Tada and Smith, 2001). Much of our current understanding of the critical role of T-box genes comes from the analysis of phenotypes produced by genetic mutations. Importantly, several TBX genes are causally implicated in human congenital malformations. For example, the cardiovascular defects in DiGeorge syndrome are caused by haploinsufficiency of *TBX1* (Merscher et al., 2001); the ulnar-mammary syndrome is a pleiotropic disorder characterized by defects in limb, apocrine gland, tooth and genital development because of haploinsufficiency of *TBX3* (Bamshad et al., 1997); and Holt-Oram syndrome, a developmental disorder of upper limb malformation and cardiac septation defects, is associated with haploinsufficiency of *TBX5* (Li et al., 1997; Bruneau et al., 2001).

The family of T-box transcription factors shares a phylogenetically conserved DNA-binding domain, which is required for specific DNA sequence recognition. The functional activity of these genes are mediated by binding to their cognate regulatory sites within the promoter and enhancer regions of genes, leading to the activation or repression of gene expression depending upon the type of T-box gene and the context within the promoter (Carreira et al., 1998; He et al., 1999; Sinha et al., 2000; Tada and Smith, 2001). Members of this gene family have been shown to have selective patterns of expression and play many key roles in patterning and specifying the development of a variety of tissues (Basson et al., 1999; Merscher et al., 2001; Lamolet et al., 2001; Bruneau et al., 2001; Tada and Smith, 2001).

We recently described a novel zebrafish T-box gene, *hrT* (*tbx20* – Zebrafish Information Network), which is expressed in the developing heart and dorsal aorta (Griffin et al., 2000; Ahn et al., 2000). *hrT* is expressed in the cardiogenic mesoderm of the anterior lateral plate from the beginning of segmentation, and continues to be expressed in the heart field until at least 72 hours (Griffin et al., 2000; Ahn et al., 2000). The onset of *hrT* expression in the lateral plate is earlier than the first expression of *nkx2.5* or *tbx5*, and coincident with the start of *nkx2.7* expression (Lee et al., 1996; Begemann and Ingham, 2000). *hrT* is thus expressed during all the key stages of cardiac development, which include cardiac cell fate specification, morphogenesis, looping of the heart tube and chamber formation (Srivastavia and Olson, 2000; Yelon et al., 1999; Stainier, 2001). In addition, *hrT* begins to be expressed in the dorsal aorta at the 15-somite stage, in addition to sites of expression in the hindbrain, eye and at the anal opening (Griffin et al., 2000; Ahn et al., 2000).

To investigate the developmental role of *hrT*, we used *hrT*-specific morpholino antisense oligonucleotides to produce zebrafish with a reduced amount of HrT. We find that *hrT* plays an important role in the later development of the heart, including normal cardiac looping and the division of the cardiac chambers. Specifically, we show that *hrT* is required to regulate *tbx5* expression levels correctly during the stages of cardiac looping. In addition, we find that *hrT* is required for the morphogenesis of the dorsal aorta, resulting in embryos lacking blood circulation. Interestingly, the vascular defects in *hrT* morphant embryos are similar to midline mutants such as *floating head* (*flh*), which we show lack expression of *hrT* in vascular progenitors. Taken together, these data indicate that *hrT* helps to mediate essential functions in vascular morphogenesis downstream of the midline mesoderm. This study provides the first demonstration of the crucial role for *hrT* in cardiovascular development and sheds new insight into the mechanism regulating the expression of *tbx5* during cardiogenesis.

MATERIALS AND METHODS

Embryos and morpholino oligonucleotide injections

Zebrafish embryos were obtained by natural spawning of adult AB strain zebrafish. Embryos were raised and maintained at 28.5°C in system water and staged as described (Westerfield, 1995). Morpholino antisense oligonucleotides were purchased from Gene-Tools (Corvallis, OR). A stock solution was prepared as described (Nasevicius and Ekker, 2000). At the one-cell stage, each embryo was injected with approximately 1 nl volume of morpholino oligonucleotide (0.2 to 5.0 ng) using a Picospritzer II (Parker Hamnifin Corporation). Embryos were collected at the appropriate stages and fixed in 4% paraformaldehyde, pH 7.0, in phosphate-buffered saline (PBS), overnight at 4ºC. Fixed embryos were dechorionated, washed three times with PBS and stored in methanol at –20ºC.

In situ hybridization

Whole-mount in situ hybridization was performed using digoxigenin-labeled antisense RNA probe and visualized using anti-digoxigenin Fab fragments conjugated with alkaline phosphatase (Roche Molecular Biochemicals) as described (Griffin et al., 1998). Riboprobes were made from DNA templates, which were linearized and transcribed with either SP6 or T7 RNA polymerase. Embryos were processed and hybridized as described (Griffin et al., 1998), except that 10 μg/ml of proteinase K in PBS/0.1% Tween-20 was used for 10 to 30 minutes depending the age of the collected embryos.

Whole-mount immunostaining

Whole-mount immunostaining was performed using monoclonal antibodies MF20 (generous gift of Dr Stephen Hauschka) and S46 (generous gift of Dr Frank Stockdale). Embryos were processed as previously described (Westerfield, 1995), except that the pericardium of each embryo was punctured before treatment with proteinase K using a fine gauge syringe needle. The color reaction was visualized with goat anti-mouse antibodies conjugated to horseradish peroxidase and 3,3′-Diaminobenzidine tetrahydrochloride (Polysciences).

Histology

Whole-mount in situ hybridized embryos were washed in water several times, and placed in a series of washes in 25%, 50%, 75% and 100% ethanol. The completely dehydrated embryos were cleared in acetone and then embedded in Paraplast II (Tissue Tek). Sections 7 μm thick were cut and mounted on glass with the same embedding plastic. The mounted slides were covered with coverslips and incubated at 60°C to dry.

RNA injection of *hrT-GFP* and *GFP* in the presence of hrTMO(1)

RNAs were synthesized from *Asp*718 linearized *CS2-hrT-GFP* (details available on request) and *CS2-GFP* (generous gift of Dr Jeff Miller) templates using the mMessage Machine kit (Ambion) and dissolved in RNase-free sterile water. RNA (0.1 ng) was injected in the presence or absence of 1.5 ng hrTMO(1) into one cell zebrafish embryos. The expression of *hrT-GFP* and *GFP* were analyzed at the shield stage using green fluorescent microscopy.

Overexpression of an inducible *hrT* expression plasmid

Synthetic capped mRNA transcripts were synthesized by SP6 in vitro transcription (mMessage machine; Ambion) of an *Asp*718 linearized CS2 template containing an insert of the coding region of *hrT* fused to the glucocorticoid receptor ligand binding domain (*GR-hrT*; details available on request). *GR-hrT* mRNA was dissolved in RNase-free sterile water and 1 nl volume of RNA at a concentration of 0.2 mg/ml was injected into one cell zebrafish embryos. The GR-hrT protein was activated by adding 0.1% volume of 100 mM dexamethasone in 100% ethanol to give a final concentration of 100 μM dexamethasone. Control treated embryos were put into 0.1% ethanol at the same time.

Photography and image processing

For photography, whole-mount in situ hybridized embryos were post-fixed in 4% paraformaldehyde, washed three times with PBS, dehydrated with methanol, cleared in methyl salicylate and mounted onto a glass slide with Permount as described (Melby et al., 1997). Plastic tissue sections and whole-mount in situ hybridized embryos were photographed on an Axioplan microscope (Zeiss) using a digital camera (Dage). Photo images were cropped and assembled using the Photoshop program version 5.5 (Adobe).

RESULTS

hrT inhibition causes cardiovascular defects

To determine the role of *hrT* in zebrafish development, we designed a morpholino antisense oligonucleotide (Nasevicius and Ekker, 2000; Heasman et al., 2000), hrTMO(1), that was designed to block the translation of *hrT* (Fig. 1A). In addition, we designed a control morpholino antisense oligonucleotide, Control-MO, which is a modified sequence of hrTMO(1) with four nucleotide changes (Fig. 1A). At 1.5 ng/embryo of hrTMO(1), we consistently obtained morphants that were generally normal except that they had dysmorphic hearts, cardiac edema, no blood circulation (65%, n=100), while injection of the same amount of Control-MO produced a severely attenuated effect (Table 1), demonstrating that these results were not due to an injection artifact. In addition, these phenotypes were not observed after injection of over ten other morpholino oligonucleotides (Lee and Kimelman, 2002) (K. Griffin and D. K., unpublished; S. Chen and D. K., unpublished; W. Clements and D. K., unpublished).

The abnormal cardiac development was visible in hrTMO(1)-injected zebrafish embryos at 24 hours post fertilization (hpf) (Fig. 1B,C). By 48 hpf, the heart tube of uninjected zebrafish embryos developed into clearly separate chambers (Fig. 1F,H), whereas the heart tube in *hrT* morphants remained in a tubular structure with no obvious morphological distinction between the chambers (Fig. 1G,I). This morphological alteration was also associated with abnormal

contractility of the heart (see Movies at http://dev.biologists.org/supplemental/). The hearts of *hrT* morphants show slower cardiac rhythm than those of their uninjected siblings.

To confirm that these morphant phenotypes were specifically due to the inactivation of *hrT* function, we first investigated the efficacy of hrTMO(1) in blocking the translation of the *hrT* gene. To do this, we constructed a fusion between the coding region of *hrT* and the *GFP* reporter gene, *hrT-GFP*, which includes the binding region of hrTMO(1). Injection of 0.1 ng *hrT-GFP* RNA in the presence of 1.5 ng hrTMO(1) resulted in the absence of GFP protein expression (Fig. 1J-M; 100%, *n*=55). By contrast, there was no effect on the expression of GFP in embryos co-injected with 0.1 ng *GFP* RNA and 1.5 ng hrTMO(1) (Fig. 1N-Q; 90%, *n*=45). These experiments demonstrate that hrTMO(1) is able to specifically block the translation of the *hrT* gene via the binding sequence for hrTMO(1). To demonstrate further the morphant phenotypes were the result of specific loss of the *hrT* gene function, we designed a second morpholino oligonucleotides, hrTMO(2), which binds to the *hrT* transcript at a different region than hrTMO(1) (Fig. 1A). At a range of 6.0 to 12.5 ng, the hrTMO(2)-injected zebrafish embryos exhibited the same phenotype as that observed with hrTMO(1) (Fig. 1D,E), and the resulting phenotypes were dose dependent (Table 1). At higher doses, both morpholino oligonucleotides caused nonspecific effects (data not shown). Thus, we conclude that the specific morphant phenotypes produced by hrTMO(1) result from the specific inhibition of HrT.

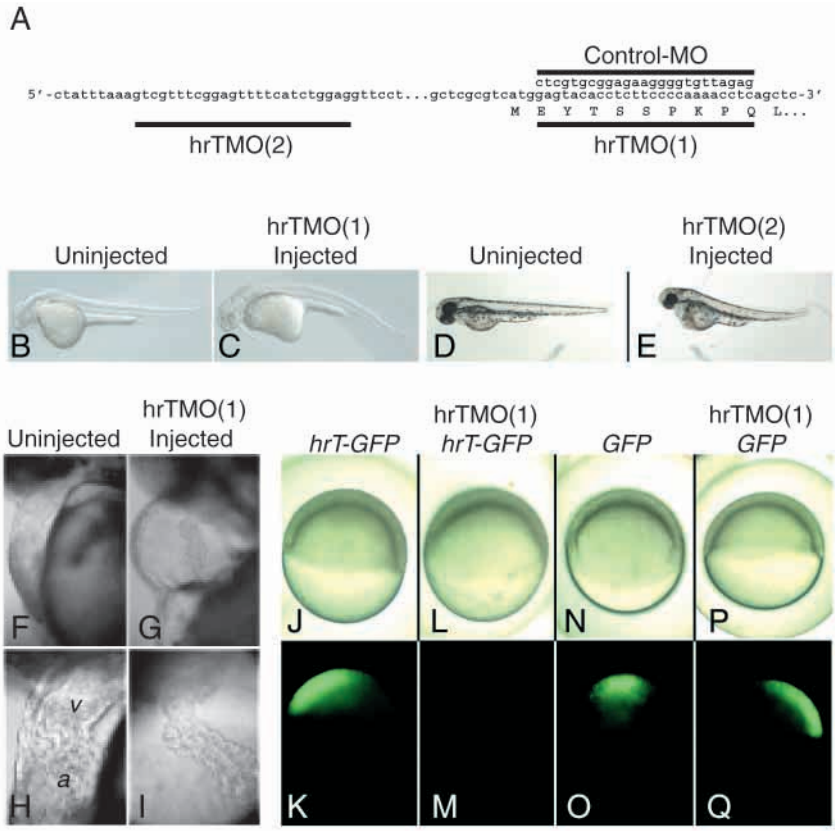

Fig. 1. *hrT* morphant phenotypes. (A) Binding positions of the morpholino antisense oligonucleotides, hrTMO(1) and hrTMO(2), to the *hrT* transcript. The sequence of the control-MO is also shown. (B-E) Lateral views with anterior towards the left. (B,C) The overall morphology of an uninjected (B) and hrTMO(1)-injected (C) embryos at 24 hpf. (D,E) The overall morphology of an uninjected (D) and hrTMO(2)-injected (E) embryos at 50 hpf. (F-I) Lateral view with anterior towards the top. (F,G) Heart morphology of uninjected embryo (F) and of hrTMO(1)-injected (G) embryo at 48 hpf. (H,I) Higher magnification of F,G, respectively (v, ventricle; a, atrium). Live (J,L,N,P) and green fluorescent (K,M,O,Q) pictures of embryos injected at the shield stage with: (J,K) 0.1 ng of *hrT-GFP* RNA; (L,M) 0.1 ng of *hrT-GFP* RNA plus 1.5 ng of hrTMO(1); (N,O) 0.1 ng of *GFP* RNA; and (P,Q) 0.1 ng of *GFP* RNA plus 1.5 ng of hrTMO(1).

Defective cardiac looping in *hrT* morphants

hrT is expressed throughout all stages of heart formation including cardiac cell fate specification, morphogenesis, looping of the heart tube and chamber formation (Griffin et al., 2000; Ahn et al., 2000). These different key stages have been well characterized with molecular markers, including *nkx2.5*, *tbx5*, *cardiac myosin light chain 2* and *ventricle myosin heavy chain* (Lee et al., 1996; Serbedzija et al., 1998; Begemann and Ingham, 2000; Yelon et al., 1999). These markers were used as in situ hybridization probes to assess gene expression changes during cardiac development in embryos injected with hrTMO(1) to determine when defects in *hrT* morphants occurred.

We first examined the pattern of *nkx2.5* expression during early cardiac development, starting from the specification of cardiac progenitors to the formation of a linear heart tube. One of the initial steps in cardiogenesis is the establishment of the

Table 1. Effect of morpholino antisense oligonucleotides

	Amount of morpholino antisense oligonucleotides injected per embryo					
	hrTMO(1)	Control-MO	hrTMO(2)			
Observed phenotypes	1.5 ng	1.5 ng	6.0 ng	8.0 ng	10.0 ng	12.5 ng
Dysmorphic heart	78%	2%	30%	44%	69%	93%
No circulating blood	65%	4%	15%	38%	47%	79%
Normal cardiovascular development	12%	94%	70%	56%	31%	7%
Total embryo number	100	98	112	102	179	109

These phenotype frequencies (%) are a representative of two or three experiments. Analysis was at 38-42 hpf.

heart field in the anterior region of the lateral plate mesoderm. These cardiac precursors are characterized by the bilateral expression of *nkx2.5* (Lee et al., 1996; Serbedzija et al., 1998). In *hrT*-morphant embryos, *nkx2.5* expression at the 12-somite stage in the anterior lateral plate mesoderm was unaffected by the depletion of *hrT*, indicating that *hrT* is not required for establishment of bilateral sets of cardiac precursors (Fig. 2A,B). Similarly, using *nkx2.5* expression to visualize the cardiac primordium, heart development appeared normal in *hrT*-morphant embryos through the stages of fusion of the bilateral heart fields and leftward jogging of the heart (Fig. 2C,D). We also compared the relative distributions of *cardiac-myosin light chain-2* (*cmlc2*), a pan-cardiac marker and *ventricular myosin heavy chain* (*vmhc*), to examine the formation of atrial and ventricular precursors (Yelon et al., 1999). At the 17-somite stage and at 24 hpf, expression of *cmlc2* and *vmhc* in injected embryos was indistinguishable from uninjected embryos, indicating that the specification of ventricular and atrial precursors proceeded normally in *hrT*-morphant embryos (data not shown). We conclude therefore that the early expression of *hrT* in cardiac precursors (up to 24 hpf) is not essential for the early differentiation or morphogenesis of the heart.

At 36 hpf, we used *cmlc2* to visualize the process of cardiac looping in *hrT* morphants. *cmlc2* is expressed in the atrial and ventricular regions, outlining the development of the whole heart. In uninjected embryos, the process of cardiac looping is marked by a rightward bending in the ventricular region (Fig. 2E). This morphological signature of cardiac looping was not observed in *hrT* morphants (Fig. 2F). Thus, HrT plays an essential role in cardiac morphogenesis that is not evident until the cardiac looping stage, significantly later than the onset of *hrT* expression in cardiac precursors.

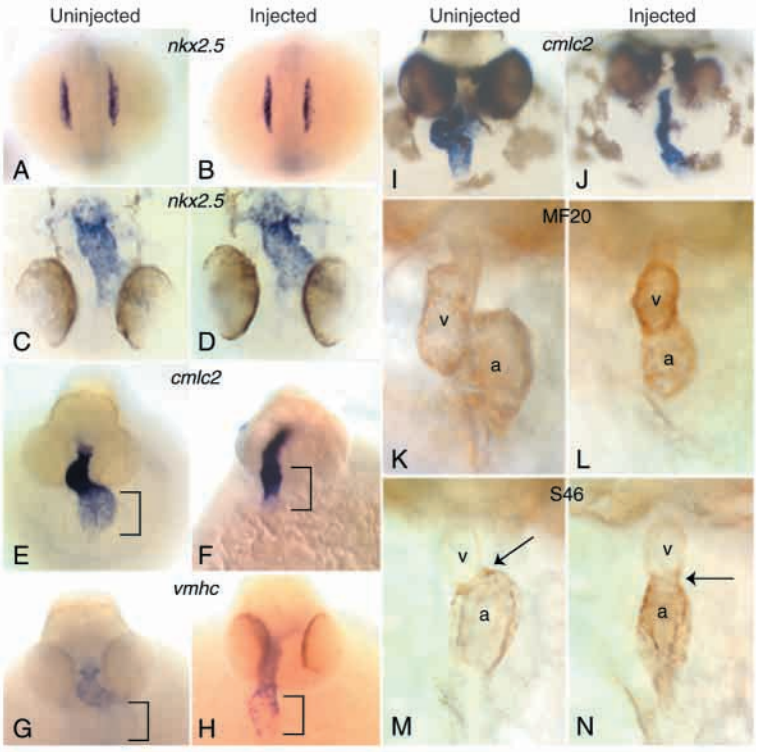

Fig. 2. In situ and immunohistological analysis of cardiogenesis in the *hrT* morphants. (A-D) Dorsal views with anterior at the bottom. (A,B) Expression of *nkx2.5* in uninjected (A) and hrTMO(1)-injected (B) embryos at the 12-somite stage in bilateral stripes. (C,D) Expression of *nkx2.5* in the linear cardiac tube of uninjected (C) and hrTMO(1)-injected (D) embryos at 24 hpf. (E-N) Frontal views with anterior towards the top. (E,F) Cardiac expression pattern of *cmlc2* in uninjected (E) and hrTMO(1)-injected (F) embryos at 33 hpf. Black bracket indicates the atrial region. (G,H) Cardiac expression patterns of *vmhc* in uninjected (G) and hrTMO(1)-injected (H) embryos at 33 hpf. Black bracket marks the atrial region. (I,J) Expression of *cmlc2* in uninjected (I) and hrTMO(1)-injected (J) embryos at 36 hpf when cardiac looping is taking place. The injected embryo (J) has defective looping. (K,L) MF20 antibody stains the atrium and ventricle of uninjected (K) and hrTMO(1)-injected (L) embryos at 48 hpf. (M,N) S46 antibody stains the atrium of uninjected (M) and hrTMO(1)-injected (N) embryos at 48 hpf. Black arrows indicate the atrioventricular boundary. (a, atrium; v, ventricle). Injected embryos were injected with 1.5 ng of hrTMO(1).

Abnormal cardiac chamber formation in *hrT* morphants

In addition to the absence of looping, the distribution of *cmlc2* expression at 36 hpf also revealed a defect in chamber morphology. In uninjected embryos, the dense *cmlc2* expression observed in the ventricle contrasts with the relatively diffuse appearance of the atrium (Fig. 2E). In injected embryos, however, atrial expression of *cmlc2* appeared similar to ventricular expression (Fig. 2F). This defect could either be due to collapse of the atrium, so that there was an apparent increase in the density of *cmlc2* expression there, or because atrial chamber identity was defective. Consistent with the latter possibility, we observed that *vmhc* expression in *hrT* morphants was no longer specific to the ventricle and was now also detected in the atrium (Fig. 2G compare with 2H), suggesting that *hrT* may play a role in maintaining chamber-specific patterns of gene expression.

At 48 hpf, when morphologically distinct cardiac chambers begin to form in untreated embryos, *hrT* morphants did not exhibit clearly distinct physical boundaries between the chambers. To examine the chamber identity in *hrT* morphants, we analyzed cardiac chamber formation using the monoclonal antibodies MF20 to detect a myosin chain common to both chambers (Fig. 2K), and S46 which detects an atrial-specific myosin epitope (Fig. 2M) (Yelon et al., 1999; Evans et al., 1988). Staining of the *hrT* morphants with MF20 indicated the presence of two distinct chambers (Fig. 2L). This result was confirmed with the atrium-specific antibody S46, which revealed a clear atrioventricular boundary (Fig. 2N). Despite the absence of morphologically distinct cardiac chambers in the *hrT* morphants, the heart was characteristically divided into an atrium and ventricle at this stage. Thus, the depletion of *hrT* function does not prevent the acquisition of anteroposterior fates within the heart tube, although there are clear alterations to gene expression within the atrium.

Regulation of *tbx5* by HrT

Our initial study of *hrT* suggested that it might be genetically upstream of *tbx5* as the expression of *hrT* precedes the

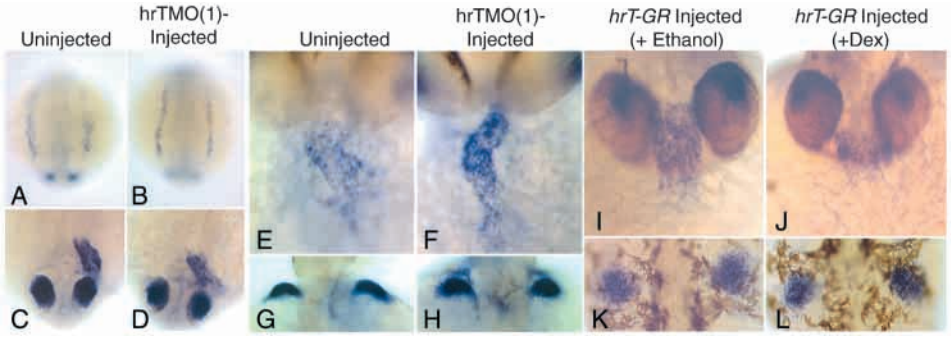

Fig. 3. HrT regulates *tbx5*. (B,D,F,H) Embryos injected with 1.5 ng hrTMO(1) are compared with uninjected (A,C,E,G) embryos. (A-D) Dorsal views with anterior towards the bottom. (A,B) Expression of *tbx5* at the 15-somite stage. (C,D) Expression of *tbx5* at 24 hpf in the heart field. (E,F) Frontal views with anterior towards the top shows the expression of *tbx5* at 33 hpf in the heart field. Note increased expression of *tbx5* in hrTMO(1)-injected embryos (F). (G,H) Dorsal views with anterior to the top shows the expression of *tbx5* at 33 hpf in the fin buds. (I-L) Embryos were injected with 0.2 ug of *hrT-GR* RNA and half were treated with dexamethasone (Dex) as indicated. (I,J) Frontal views with anterior to the top of 30 hpf embryos showing *tbx5* expression in the heart. Note decreased *tbx5* expression after GR-hrT induction. (K,L) Dorsal views with anterior towards the top of 30 hpf embryos, showing the expression of *tbx5* in the developing fin buds. GR-hrT induction did not change the fin bud expression of *tbx5*.

expression of *tbx5* in the heart field (Griffin et al., 2000). Consistent with this idea, mice lacking the *tbx5* gene have normal expression of *tbx20*, the mouse ortholog of *hrT* (Bruneau et al., 2001). Because *tbx5* is a key transcription factor that regulates cardiac morphogenesis and gene expression within the heart field (Basson et al., 1999; Horb and Thomsen, 1999; Bruneau et al., 2001), we wished to determine the relationship between HrT and *tbx5* expression. In *hrT* morphants at 33 hpf, we observed a dramatic upregulation of *tbx5* expression in the embryonic heart (Fig. 3E,F; 44%, *n*=34). However, there was no change in *tbx5* expression at earlier times (Fig. 3A-D), or in the developing pectoral fin buds where *tbx5* is expressed but *hrT* is not (Fig. 3G,H).

As depletion of HrT increased the expression levels of *tbx5* in the heart, we predicted that overexpression of *hrT* would decrease the expression of *tbx5*. In order to regulate the expression of *hrT*, we constructed a fusion between the coding region of *hrT* and the ligand-binding domain of the *glucocortiocoid receptor* (*GR-hrT*; *gr* – Zebrafish Information Network). As shown previously, these fusion proteins are inactive until the hormone dexamethasone is added (Kolm and Sive, 1995; Tada et al., 1997). For the experiments shown here, dexamethasone was added at the 12-somite stage (Fig. 3I-L), but the same results were observed when the hormone was added at earlier stages (data not shown). We also determined that the same concentration of dexamethasone does not cause any apparent developmental defect in the developing uninjected embryos (data not shown). Induction of GR-HrT had no effect on the morphological appearance of the heart field or on the expression of *tbx5* before the stages of cardiac looping (data not shown). However, at 30 hpf, we observed a significant downregulation of *tbx5* expression in the embryos after induction of GR-HrT (Fig. 3I,J; 55%, *n*=40), as well as morphological alterations in the heart at later stages. While the hearts of control embryos underwent the normal process of heart looping, the hearts in GR-HrT-induced embryos did not loop (data not shown). The effects of *hrT* overexpression on *tbx5* were specific to the heart, as the levels of *tbx5* expression in the fin buds of both GR-HrT-induced and control embryos were the same (Fig. 3K,L). Both the overexpression and the morpholino antisense experiments demonstrate that HrT acts to regulate the levels of *tbx5* expression during the stages of cardiac looping. As normal cardiac morphogenesis and gene expression requires a precise regulation of the levels of *tbx5* (reviewed by Hatcher and Beeson, 2001), our results suggest that a major role for HrT is to modulate the levels of *tbx5* during cardiac looping.

The role of *hrT* in hematopoiesis

In addition to the defective heart, *hrT* morphants do not have circulating blood. To determine the cause of this defect, we examined the process of hematopoiesis and vasculogenesis in embryos depleted of *hrT* function. Hematopoiesis occurs in several waves and in distinct locations, giving rise to the terminal differentiation of various hematopoietic progenitor cells, including early macrophages, erythrocytes, megakaryocytes and leucocytes (Zon, 1995; Herbomel et al., 1999; Detrich et al., 1995; Thompson et al., 1998). From the onset of gastrulation to 24 hpf in the *hrT* morphants, we observed no apparent change in the expression of genes that are known to denote the development of different hematopoietic cell lineages (data not shown), indicating that the different hematopoietic cell lineages form in the absence of *hrT* function. Thus, the absence of circulating blood is not a result of an absence of blood, but is most probably due to a problem with vasculogenesis. This conclusion is supported by the observed blood pooling in the peri-anal region of the *hrT* morphants at 36 hpf (Fig. 4F). Although the hematopoiesis in the *hrT* morphants was essentially normal, we did observe an interesting alteration in the pattern of *gata1* and *gata2* expression. At the 2- to 12-somite stage, *gata1* expression resides in two stripes flanking the posterior paraxial mesoderm in the developing zebrafish embryos, marking the erythrocyte and megakaryocyte lineages (Detrich et al., 1995). At the 8- to 10-somite stage, we found a ‘U’-shaped pattern of *gata1* expression in *hrT* morphants, rather than the bilateral stripes of expression in the uninjected sibling embryos, because of ectopic expression of *gata1* in the most posterior lateral plate mesoderm (Fig. 4B; 61%, *n*=81). We observed a similar result for *gata2* expression, which marks all of the definitive hematopoietic lineages (data not shown). Interestingly, *hrT* is expressed in the most posterior region of the lateral plate where the normal bilateral stripes join to form the ‘U’-shaped pattern in the *hrT* morphants (Fig. 4C,D), suggesting that HrT normally prevents the hematopoietic fate in this domain.

The role of *hrT* in vasculogenesis

hrT is expressed in the dorsal aorta (Griffin et al., 2000; Ahn

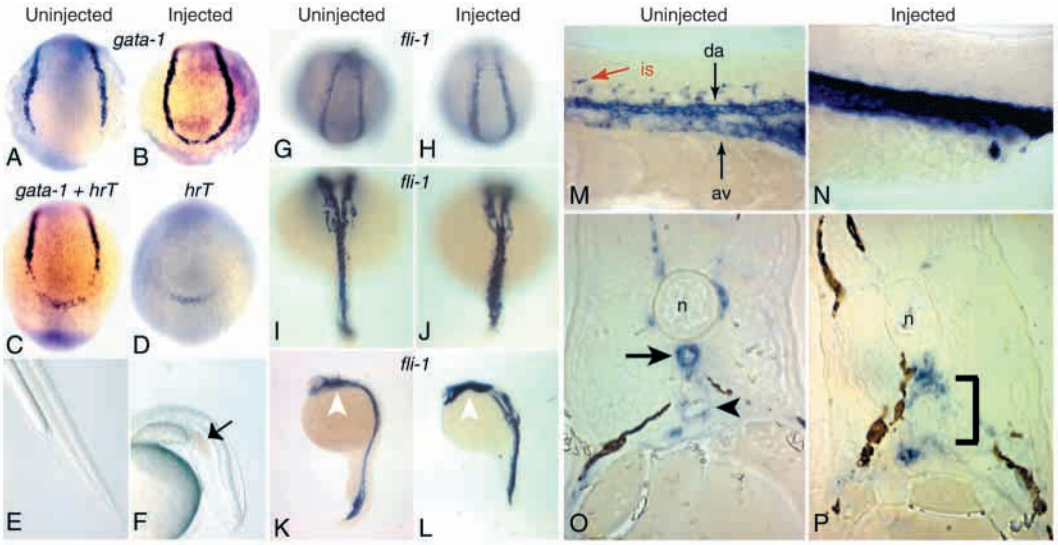

Fig. 4. Analysis of gene expression during hematopoiesis and the formation of the trunk vasculature. (A-D) 8- to 10-somite stage embryos; posterior views with dorsal to the top. (A,B) Expression of *gata1* in uninjected (A) and hrtMO(1)-injected (B) embryos. Note that injected embryos express *gata1* in the most posterior region of the embryo, in contrast to uninjected embryos. (C) Expression of *hrT* and *gata1* in uninjected embryo. (D) Expression of *hrT* in hrTMO(1)-injected embryo. The same expression pattern is found in uninjected embryos (not shown). Note that the *hrT* expression domain coincides with the region of ectopic *gata1* expression in the morphants (B). (E,F) Live pictures of the posterior half of uninjected (E) and hrTMO(1)-injected (F) embryos at 36 hpf. Arrow indicates the blood pooling in the peri-anal region of the injected embryos. (G,H) Posterior views with dorsal towards the top. *fli1* is expressed in a 'U-shaped pattern at 14 hpf in uninjected (G) and hrTMO(1)-injected (H) embryos. (I,J) Dorsal views with anterior towards the top. Expression of *fli1* at 20 hpf. In uninjected embryos, *fli1*-expressing cells are at the midline (I), whereas *fli1*-expressing cells have not converged completely to the midline in *hrT* morphants (J). (K,L) Lateral views with anterior towards the top. The expression pattern of *fli1* in uninjected (K) and hrTMO(1)-injected embryos at 24 hpf. White arrowhead indicates the *fli1* expression in the pharyngeal primordium. (M,N) Lateral views of 24 hpf embryos with anterior towards the left. In uninjected embryos (M), *fli1* expression is apparent in the dorsal aorta (da), axial vein (av) and intersegmental vessels (is), whereas *hrT* morphants (N) exhibit a single domain of *fli1* expression in the midline of the entire trunk with no intersegmental vessels. (O,P) Transverse sections of embryos at 30 hpf stained with *fli1*, dorsal towards the top. In uninjected embryos (O), the formation of the dorsal aorta (black arrow) below the notochord (n) and axial vein (black arrowhead) is apparent. In the *hrT* morphants (P), only a single lumen is present. The black bracket indicates the developing region of the dorsal aorta and axial vein. Injected embryos were injected with 1.5 ng of hrTMO(1).

et al., 2000), and thus the blood circulation defects could be due to aberrant formation of the dorsal aorta. To determine if there is a vascular defect when *hrT* function is impaired, we investigated the formation of the major blood vessels in the *hrT* morphants. After gastrulation, vasculogenesis begins with the formation of two stripes of endothelial precursors at the lateral edges of the mesoderm, and these cells express *fli1*, a member of the ETS-domain family of transcription factors (Brown et al., 2000). At 14 hpf, the expression of *fli1* in the lateral mesoderm extends along the entire axis during segmentation in two continuous bands, forming a 'U'-shaped surrounding the axial and paraxial mesoderm (Fig. 4G). At this stage, we found that the pattern of *fli1* expression was normal in *hrT* morphants when compared with that in the uninjected siblings (Fig. 4G,H). This result suggests that the early specification of endothelial precursors is unaffected when *hrT* function is disrupted. At approximately 20 hpf, the 'U'-shaped pattern of *fli1* expression in trunk and tail coalesces in the midline (Fig. 4I). Subsequently, the *fli1* expression is found in the walls of major vessels, including the dorsal aorta, axial vein and intersegmental vessels (Fig. 4K). At 20 hpf, the expression of *fli1* was detected in a broad distribution pattern around the midline of *hrT* morphants (Fig. 4J), suggesting that the fusion of endothelial cells to form the dorsal aorta in the midline was disrupted. By 24 hpf, the abnormal expression pattern of *fli1* in *hrT* morphants was even more apparent. In uninjected embryos, the *fli1* expression was detected in the dorsal aorta, axial vein and intersegmental vessels (Fig. 4M), whereas in *hrT* morphants, *fli1* was expressed in a single domain running along the midline ventral to the notochord (Fig. 4N; 53%, *n*=30). In addition, the sprouting of intersegmental vessels was not detected in *hrT* morphants (Fig. 4N). However, the pattern of *fli1* expression in the pharyngeal primordium appeared to be normal (Fig. 4K,L), suggesting that the vasculogenic requirement for *hrT* is localized to the trunk of the embryos.

In sections of *fli1*-stained, uninjected embryos, the dorsal aorta is seen ventral to the notochord and the axial vein is below the aorta (Fig. 4O). In the *hrT* morphants, the *fli1*-expressing cells have not organized into two clear vessels, although we typically saw one lumen above the gut tube (Fig. 4P). As *hrT* is expressed in the dorsal aorta but not the axial vein, we expect that the major defect is due to the formation of this vessel. Thus, we conclude that the failure of *hrT* morphants to circulate blood is primarily due to a defect in the formation of the dorsal aorta.

HrT is a potential downstream effector of *flh*

We noticed a strong resemblance between the trunk vascular defects in the *hrT* morphants and *floating head* (*flh*) mutant embryos (Sumoy et al., 1997; Brown et al., 2000; Fouquet et al., 1997). *flh* is a homeodomain transcription factor expressed in the notochord precursors, and the *flh* mutation causes an absence of notochord (Talbot et al., 1995). In *flh* mutants as in the *hrT* morphants, blood circulation does not occur, and the blood accumulates in the peri-anal region because of a failure to form the dorsal aorta (Fouquet et al., 1997; Brown et al., 2000; Sumoy et al., 1997). Similarly in the *hrT* morphants and

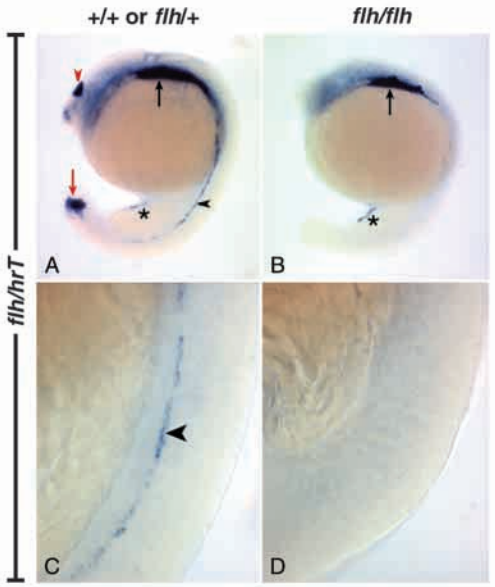

Fig. 5. The expression of *flh* and *hrT* in *flh* mutant embryos. (A-D) Lateral views of 17-somite embryos with anterior towards the top, hybridized with a mixture of *flh* and *hrT* probes. In wild-type embryos or *flh* heterozygotes (A), *flh* is expressed in the tip of the tail (red arrow) and epiphysis (red arrowhead), and *hrT* is expressed in the dorsal aorta (black arrowhead), ventral region of the gut tube (asterisk) and in the heart (black arrow). In *flh* homozygotes (B), *flh* expression is absent and *hrT* expression is missing in the dorsal aorta. The gut tube and cardiac expression of *hrT* is not affected. (C,D) Higher-power views of the embryos in A,B, respectively. (C) The dorsal aorta expression of *hrT* (black arrowhead) in a wild-type or *flh* heterozygote. (D) The complete absence of *hrT* expression in the dorsal aorta of a homozygous *flh* embryo.

flh mutants, *fli1* is expressed in a single stripe in the midline with no apparent intersegmental vessels.

The similarity between the vascular defects in *flh* mutant embryos and *hrT* morphants, prompted us to examine *hrT* expression in *flh* embryos. In *flh* homozygotes, which were identified morphologically and confirmed by the absence of *flh* expression (Talbot et al., 1995), we observed a complete absence of *hrT* expression in the vascular progenitors whereas other domains of *hrT* expression were unaffected (Fig. 5). This is consistent with the possibility that *hrT* expression in vascular progenitors depends, directly or indirectly, upon a signal from the midline mesoderm

DISCUSSION

Using two non-overlapping *hrT*-specific morpholino antisense oligonucleotides, we have demonstrated that *hrT* is required for normal heart development. Prior to the onset of cardiac looping, cardiogenesis progressed normally in *hrT* morphants, indicating that there is no requirement for *hrT* function in the early stages of heart development. We first began to see the effect of depleting HrT function around 33 hpf. In *hrT* morphants, the embryonic heart showed no ventricle bending, a characteristic of normal cardiac looping. In addition, the expression of two marker genes, *cmlc2* and *vmhc* was aberrant, with abnormal expression of these genes in the atrium. Although the dysmorphic hearts in the *hrT* morphants appeared to form two distinct chambers, the heart remained as a linear tube and did not form the characteristically looped structure, resulting in a heart with abnormal contractions and a slower rhythm.

Although *hrT* is expressed very early in the heart field, depletion of its function did not have an apparent effect until 33 hpf. It is possible that this is due to incomplete inhibition of *hrT* function using the antisense oligonucleotides or due to the presence of a gene that compensates at earlier times for a loss of *hrT*. However, it is intriguing that a similar effect has been observed with murine *tbx5*; while *tbx5* is also expressed very early in the heart field (Liberatore et al., 2000), elimination of the *tbx5* gene did not have an effect until later times of development (Brunneau et al., 2001). This finding suggests that the T-box genes may not function by themselves in the regulation of heart development, but may need to interact with other factors that are expressed at later times of development.

Regulatory role of *hrT* during cardiogenesis

A key finding in this study is that HrT acts as a regulator of *tbx5* expression. Depletion of HrT function causes the cardiac expression of *tbx5* to be upregulated, whereas overexpression of *hrT* leads to the downregulation of *tbx5* expression in the developing heart. Importantly, in both cases, the regulation of *tbx5* was specific to the heart and did not affect the expression of *tbx5* in the limb buds. Although we do not yet know whether or not Tbx5 regulates *hrT* expression in zebrafish, mice lacking the *tbx5* gene do not show alterations in the expression of the murine *hrT* ortholog *tbx20* (Brunneau et al., 2001), indicating that *hrT* may function solely upstream of *tbx5*.

tbx5 has emerged as a key gene regulating heart development from amphibians to mammals (Horb and Thomsen, 1999; Liberatore et al., 2000; Bruneau et al., 2001). Patients with Holt-Oram syndrome, a disorder caused by haploinsufficiency of the *tbx5* gene, have a high penetrance of cardiac defects (Li et al., 1997; Basson et al., 1999). Similar defects have been found in mice lacking one copy of the *tbx5* gene (Bruneau et al., 2001). Mice lacking both copies of *tbx5* have more severe defects, including an absence of heart looping and alterations in a subset of cardiac-specific genes, although the early steps in cardiac development appear normal (Bruneau et al., 2001). Curiously, mice overexpressing *tbx5* also have cardiac looping defects as well as alterations in the expression of some cardiac genes (Liberatore et al., 2000). These results indicate that the gene dose of *tbx5* is crucial for normal cardiac morphogenesis (Bruneau et al., 2001; Hatcher and Basson, 2001). These studies fit very well with our observations that inhibition of *hrT* function or overexpression of *hrT*, which cause an increase or decrease of *tbx5* expression, respectively, leads to defects in cardiac morphogenesis. Importantly, zebrafish *tbx5* mutants also show a complete absence of heart looping (M. Fishman, personal communication). It will be of great interest to determine if the alterations we observed in cardiac development are due solely to changes in the level of *tbx5* expression, or whether *hrT* has additional *tbx5*-independent functions in the heart.

The role of *hrT* in the hematopoiesis and vasculogenesis

Another key aspect of *hrT* depletion is the absence of

circulating blood. By examining the expression of a variety of different blood cell markers at various stages in *hrT* morphants, we find that there is no observable defect in hematopoiesis. In analyzing vasculogenesis, however, we have observed abnormal trunk vascular development in the *hrT* morphants. In *hrT* morphants, the endothelial marker *fli1* is expressed normally at 14 hpf when endothelial cells form a 'U'-shape around the axial and paraxial mesoderm, demonstrating that *hrT* plays no significant role in the specification of endothelial cells. At 24 hpf, the trunk vascular defect is evident by the altered expression of *fli1*, as well as the absence of normal trunk vessel formation. In addition, no intersegmental vessels sprout from the domain of the aberrant *fli1* expression. As *hrT* is expressed only in the dorsal aorta (Griffin et al., 2000; Ahn et al., 2000), we suggest that *hrT* is required specifically in the dorsal aorta rather than the axial vein, although we do not rule out the possibility of indirect effects on axial vein formation due to a defective dorsal aorta. As the endothelial cells come close to the midline in *hrT* morphants but do not completely fuse to give the dorsal aorta, our results suggest that *hrT* plays a critical role in assembling the endothelial cells into a vessel.

We noticed a striking similarity between the *hrT* morphants and *flh* mutants with regard to the formation of the vascular system, and we found that *hrT* expression is specifically eliminated in the dorsal aorta of *flh* mutants, while *hrT* expression in other regions is unaffected. As the major defect in *flh* mutants is an absence of notochord, it has been suggested that formation of the endothelial cells into the dorsal aorta requires a notochord-derived signal such as *sonic hedgehog* (*shh*) (Brown et al., 2000; Fouquet et al., 1997; Sumoy et al., 1997). Our results suggest that HrT is an essential component of the response to this signal, and indeed we have observed that *hrT* expression is abolished in the hedgehog signaling mutant *you-too* (D. P. S., K. J. P. G. and D. K., unpublished). As the process of vessel formation is still not well understood, it will be very interesting to determine the targets of HrT in the dorsal aorta.

Inhibition of gene expression by *hrT*

We observed a very interesting alteration in the expression pattern of *gata1* and *gata2* at the 8- to 10-somite stage in *hrT* morphants. While *gata1* and *gata2* are normally expressed in bilateral stripes, in *hrT* morphants, *gata1* and *gata2* form a 'U'-shaped pattern because of the presence of an extra posterior domain of expression that connects the two bilateral stripes. This extra domain of expression coincides with a region of the embryo that expresses *hrT* (Griffin et al., 2000; Ahn et al., 2000), indicating that one function of *hrT* is to prevent the expression of *gata1* and *gata2* in the most posterior lateral plate of the developing embryo. This ectopic expression of *gata1* and *gata2*, as well as the increased cardiac expression of *tbx5* and *vmhc*, suggests that an important function of HrT is to negatively regulate gene expression, at least indirectly.

A role for *hrT* in human cardiovascular disease?

This study has demonstrated a clear role for *hrT* in zebrafish cardiovascular development. Mutations in the human *hrT* ortholog, *TBX20*, are candidates for producing congenital cardiovascular defects that are among the most prevalent defects affecting live births. Since several human T-box genes have been shown to cause birth defects when haploinsufficient (Basson et al., 1999; Li et al., 1997; Bamshad et al., 1997; Merscher et al., 2001), it will be worthwhile examining the *TBX20* gene in humans with congenital heart or vascular defects if a disease allele maps to this genetic interval.

We thank Chris Bjornson and Wilson Clements for reading this manuscript; Debbie Yelon, Bernard Thisse and Adam Rodaway for probes; Stephen Hauschka and Frank Stockdale for antibodies; Jeff Miller for the *CS2-GFP* plasmid DNA; and Dave Raible for help and advice during this project. D. S. was supported by a vascular training grant (T32 07312) and a NRSA fellowship (F32 HD08725). This work was supported by grant 0078303 from the National Science Foundation to D. K.

REFERENCES

Ahn, D. A., Ruvinsky, I., Oates, A. C. and Ho, R. K. (2000). *Tbx20*, a new vertebrate T-box gene expressed in the cranial motor neurons and developing cardiovascular structures in zebrafish. *Mech. Dev*. **95**, 253-258.

Bamshad, M., Lin, R. C. and Law, D. J. (1997). Mutations in human *TBX3* alter limb, apocrine and genital development in ulnar-mammary syndrome. *Nat. Genet*. **16**, 311-315.

Basson, C. T., Huang, T., Lin, R. C., Bachinsky, D. R., Weremowicz, S., Vaglio, A., Bruzzone, R., Quadrelli, R., Lerone, M., Romeo, G. et al. (1999). Different *Tbx5* interactions in heart and limb defined by Holt-Oram syndrome mutations. *Proc. Natl. Acad. Sci. USA* **96**, 2919-2924.

Begemann, G. and Ingham, P. (2000). Developmental regulation of *Tbx5* in zebrafish embryogenesis. *Mech. Dev*. **90**, 299-304.

Brown, L. A., Rodaway, A. R. F., Schilling, T. F., Jowett, T., Ingham, P. W., Patient, R. K. and Sharrocks, A. D. (2000). Insights into early vasculogenesis revealed by expression of the ETS-domain transcription factor *Fli-1* in wild-type and mutant zebrafish embryos. *Mech. Dev*. **90**, 237-252.

Bruneau, B. G., Schmitt, J. P., Charron, F., Robitaille, L., Caron, S., Conner, D. A., Gessler, M., Nemer, M., Seidman, C. E. and Seidman, J. G. (2001). A murine model of Holt-Oram syndrome defines roles of the T-box transcription factor *Tbx5* in cardiogenesis and disease. *Cell* **106**, 709-721.

Carreira, S., Dexter, T. J., Yavuzer, U., Easty, D. J. and Goding, C. R. (1998). Brachyury-related transcription factor *Tbx2* and repression of the melanocyte-specific *TRP-1* promoter. *Mol. Cell. Biol*. **18**, 5099-5108.

Detrich, H. W., III, Kieran, M. W., Chan, F. Y., Barone, L. M., Yee, K., Rundstadler, J. A., Pratt, S., Ransom, D. and Zon, L. I. (1995). Intraembryonic hematopoietic cell migration during vertebrate development. *Proc. Natl. Acad. Sci. USA* **92**, 10713-10717.

Evans, D., Miller, J. B. and Stockdale, F. E. (1988). Developmental patterns of expression and coexpression of myosin heavy chains in atria and ventricles of the avian heart. *Dev. Biol*. **127**, 376-383.

Fouquet, B., Weinstein, B. M., Serluca, F. C. and Fishman, M. C. (1997). Vessel patterning in the embryo of the zebrafish: guidance by notochord. *Dev. Biol*. **183**, 37-48.

Griffin, K. J. P., Amacher, S. L., Kimmel, C. B. and Kimelman, D. (1998). Molecular identification of *spadetail*: regulation of zebrafish trunk and tail mesoderm formation by T-box genes. *Development* **125**, 3379-3388.

Griffin, K. J. P., Stoller, J., Gibson, M., Chen, S., Yelon, D., Stainier, D. Y. R. and Kimelman, D. (2000). A conserved role for H 15-related T-box transcription factors in zebrafish and *Drosophila* heart formation. *Dev. Biol*. **218**, 235-247.

Hatcher, C. J. and Basson, C. T. (2001). Getting the T-box dose right. *Nat. Med.* **7**, 1185-1186.

He, M. L., Wen, L., Campbell, C. E., Wu, J. Y. and Rao, Y. (1999). Transcription repression by Xenopus ET and its human ortholog *TBX3*, a gene involved in ulnar-mammary syndrome. *Proc. Natl. Acad. Sci. USA* **96**, 10212-10217.

Heasman, J., Kofron, M. and Wylie, C. (2000). Beta-catenin signaling activity dissected in the early Xenopus embryo: a novel antisense approach. *Dev. Biol*. **222**, 124-134.

Herbomel, P., Thisse, B. and Thisse, C. (1999). Ontogeny and behaviour of early macrophages in the zebrafish embryo. *Development* **126**, 3735-3745.

Horb, M. E. and Thomsen, G. H. (1999). *Tbx5* is essential for heart development. *Development* **126**, 1739-1751.

Kolm, P. J. and Sive, H. L. (1995). Efficient hormone-inducible protein function in *Xenopus laevis*. *Dev. Biol*. **171**, 267-272.

Lamolet, B., Pulichino, A., Lamonerie, T., Gauthier, Y., Brue, T., Enjalbert, A. and Drouin, J. (2001). A pituitary cell-restricted T box factor, *Tpit*, activates *POMC* transcription in cooperation with Pitx homeoproteins. *Cell* **104**, 849-859.

Lee, H. and Kimelman, D. (2002). A dominant-negative form of p63 is required for epidermal proliferation in zebrafish. *Dev. Cell* **2**, 607-616.

Lee, K., Xu, Q. and Breitbart, R. E. (1996). A new-related gene, *nkx2.7*, anticipates the expression of *nkx2.5* and *nkx2.3* in zebrafish heart and pharyngeal endoderm. *Dev. Biol*. **180**, 722-731.

Li, Q. Y., Newbury-Ecob, R. A., Terrett, J. A., Wilson, D. I., Curtis, A. R., Yi, C. H., Gebuhr, T., Bullen, P. J., Robson, S. C. and Strachan, T. (1997). Holt-Oram syndrome is caused by mutations in *TBX5*, a member of the *Brachyury* (*T*) gene family. *Nat. Genet*. **15**, 21-29.

Liberatore, C. M., Searcy-Schrick, R. D. and Yutzey, K. E. (2000). Ventricular expression of *tbx5* inhibits normal heart chamber development. *Dev. Biol*. **223**, 169-180.

Melby, A. E., Kimelman, D. and Kimmel, C. B. (1997). Spatial regulation of *floating head* expression in the development notochord. *Dev. Dyn*. **209**, 2225-2237.

Merscher, S., Funke, B., Epstein, J. A., Heyer, J., Puech, A., Lu, M. M., Xavier, R. J., Demay, M. B., Russell, R. G., Factor, S. et al. (2001). *Tbx1* is responsible for cardiovascular defects in velo-cardio-facial/diGeorge syndrome. *Cell* **104**, 619-629.

Nasevucius, A. and Ekker, S. C. (2000). Effective targeted gene 'knockdown' in zebrafish. *Nat. Genet*. **26**, 216-220.

Nasevicius, A., Larson, J. and Ekker, S. C. (2000). Distinct requirements for zebrafish angiogenesis revealed by a *VEGF-A* morphant. *Yeast* **17**, 294-301.

Papaioannou, V. A. and Silver, L. M. (1998). The T-box gene family. *BioEssays* **20**, 9-19.

Serbedzija, G. N., Chen, J. and Fishman, M. C. (1998). Regulation in the heart field of zebrafish. *Development* **125**, 1095-1101.

Sinha, S., Abraham, S., Gronostajski, R. M. and Campbell, C. E. (2000). Differential DNA binding and transcription modulation by three T-box proteins, T, TBX1 and TBX2. *Gene* **258**, 15-29.

Srivastava, D. and Olson, E. N. (2000). A genetic blueprint for cardiac development. *Nature* **407**, 221-226.

Stainier, D. Y. (2001) Zebrafish genetics and vertebrate heart formation. *Nature* **2**, 39-47.

Sumoy, L., Keasey, J. B., Dittman, T. D. and Kimelman, D. (1997). A role for notochord in axial vascular development revealed by analysis of phenotype and the expression of *VEGR-2* in zebrafish *flh* and *ntl* mutant embryos. *Mech. Dev*. **63**, 15-27.

Tada, M. and Smith, J. C. (2001). T-targets: clues to understanding the functions of T-box proteins. *Dev. Growth Differ.* **43**, 1-11.

Tada, M., O'Reilly, M. A. and Smith, J. C. (1997). Analysis of competence and of *Brachyury* autoinduction by use of hormone-inducible *Xbra*. *Development* **124**, 2225-2234.

Talbot, W. S., Trevarrow, B., Halpern, M. E., Melby, A. E., Farr, G., Postlethwait, J. H., Jowett, T., Kimmel, C. B. and Kimelman, D. (1995). A homeobox gene essential for zebrafish notochord development. *Nature* **378**, 150-157.

Thompson, M. A., Ransom, D. G., Pratt, S. J., MacLennan, H., Kieran, M. W., Detrich, H. W., III, Vail, B., Huber, T. L., Paw, B., Brownlie, A. J. et al. (1998). The *cloche* and *spadetail* genes differentially affect hematopoiesis and vasculogenesis. *Dev. Biol*. **197**, 248-269.

Westerfield, M. (1995). *The Zebrafish Book*. Eugene, OR: University of Oregon Press.

Yelon, D., Horne, S. A. and Stainier, D. Y. R. (1999). Restricted expression of cardiac myosin genes reveals regulated aspects of heart tube assembly in zebrafish. *Dev. Biol*. **214**, 23-37.

Zon, L. I. (1995). Developmental biology of hematopoiesis. *Blood* **86**, 2876-2891.